Available online at www.sciencedirect.com

ScienceDirect

Energy Procedia 58 (2014) 221 – 228

Energy Procedia

Renewable Energy Research Conference, RERC 2014

Effect of salt composition and temperature on the thermal behavior of beech wood in molten salt pyrolysis

Heidi S. Nygård*, Espen Olsen

Department of Mathematical Sciences and Technology, Norwegian University of Life Sciences, 1432 Ås, Norway

Abstract

The thermal behavior of wood particles in molten salt pyrolysis was investigated. Cylindrical beech wood particles (L = 30 mm, d = 3.5 mm) were pyrolyzed using different mixtures of molten salts (FLiNaK, $(LiNaK)_2CO_3$, $ZnCl_2$–KCl, KNO_3–$NaNO_3$) over a temperature range of 400–600 °C. The temperature at the particle center was measured during the process, and used to evaluate heating rates, reaction temperatures and devolatilization times. A general observation was that beech wood is heated faster in fluoride and carbonate melts, but the differences diminish with increasing reactor temperatures. The highest heating rates at the particle center were observed in FLiNaK (46 – 56 °C/s). The effective pyrolysis temperature at which the main decomposition of cellulose and hemicellulose takes place showed a weak dependence on reactor temperature, but no significant difference between the heating media was discovered. The devolatilization time corresponding to conversion of 95% may be empirically correlated with the power law expression $t_{dev} = Ad_p^n$. Arrhenius plots were constructed to show the exponential dependence of temperature on the parameter A. The correspondingly low activation energies (13.3 – 27.4 kJ/mol) indicate heat transfer control during the decomposition process.

Peer-review under responsibility of the Scientific Committee of RERC 2014

Keywords: Beech wood; Pyrolysis; Molten Salts; Heating rate

1. Introduction

In fast pyrolysis, biomass is heated rapidly in the absence of oxygen and converted to a mixture of liquids (pyrolysis oil), non–condensable gases and solid chars. Important process conditions for high pyrolysis oil yields are moderate reactor temperatures (~500 °C), high heating rates, short vapor residence time (2 – 3 s), and rapid quenching of the pyrolysis vapors. It is essential that the biomass particles reach optimum process temperatures before they start to decompose as exposure to lower temperatures would favor formation of charcoal.[1] This makes rapid heat transfer important in the process. There are several approaches to achieve rapid heat transfer in pyrolysis,

* Corresponding author. Tel.: +47 64 96 54 63, *E–mail address: heidi.nygard@nmbu.no*

Peer-review under responsibility of the Scientific Committee of RERC 2014
doi:10.1016/j.egypro.2014.10.432

including bubbling fluid beds, circulating and transported beds, cyclonic reactors, ablative reactors, and vacuum moving beds. A detailed description of these configurations may be found in the review of fast pyrolysis technology development by Venderbosch and Prins.[2]

A less studied approach is molten salt pyrolysis. The biomass is fed into a preheated molten salt bath where the decomposition takes place. Inorganic molten salts have very good heat transfer characteristics, large heat capacities, are very stable at high temperatures, and may be used over a wide range of temperatures, from around 120 °C to well above 1000 °C. Due to their low viscosity, they will cover the biomass particles rapidly and also infiltrate the pores, leading to a larger particle area exposed to heating by the salt.[3] A review of thermal processing of biomass in molten salts has recently been published.[4] The research reviewed includes many investigations that have not so far progressed beyond the laboratory scale. It is a relatively small research area compared with more traditional conversion methods, and there is clearly a need for more basic research on the subject.

The heat transfer characteristics of molten salts have been studied for various applications.[3] Several researchers have demonstrated an increase in reaction rates by molten carbonates in thermal processing of coal [5-7] and cellulose.[8, 9] $ZnCl_2$–KCl has been used in pyrolysis of lignin, and it is found that the yields of different phenolic compounds depend on both the molar ratio of the two salts [10] and the salt–to–lignin ratio in the reactor.[11] In the Pyrocycling process [12], a mixture of KNO_3, $NaNO_2$ and $NaNO_3$ was used as an indirect heat transfer medium in vacuum pyrolysis. Nitrates have also shown good heat transfer performance in storing thermal solar energy.[13] Molten fluoride salts have been studied as a heat transfer medium in solar power towers and nuclear power plants [14], and particularly FLiNaK has been found to have good heat transfer performance.[15]

The pyrolytic behavior of single particles is important for reactor design. The aim of this work is to study the behavior of beech wood particles in molten salt pyrolysis and gain a better understanding of molten salts as a heat transfer medium in the process. This is done by measuring particle temperatures, and use these to evaluate heating rates, reaction temperatures, and devolatilization times. In a previous study [16] we found that FLiNaK gives significantly higher heating rates compared with fluidized sand bed [17] for cylindrical beech wood particles with $d \leq 4$ mm at 500 °C. In the present work, we evaluate the effect of different salt mixtures (FLiNaK, $(LiNaK)_2CO_3$, $ZnCl_2$–KCl, KNO_3–$NaNO_3$) over a wider temperature range (400 – 600 °C).

2. Experimental section

Cylindrical beech wood particles with length (L) of 30 mm and diameter (d) of 3.5 mm were prepared from untreated wood sticks with the length parallel to the fibers. This gives an aspect ratio (L/d) well within the limit for one–dimensional (1D) internal heat transfer ($L/d > 3$) [18], and the heat transfer perpendicular to the fibers is measured. This is important because of the anisotropic nature of wood, with higher thermal conductivity parallel compared to perpendicular to the fibers.[19] The samples were dried at 105 °C for 24 h prior to the experiments in order to minimize the water content. A 1 mm type K thermocouple, placed inside a steel tube for support, was used to record the temperature T at the particle center at the frequency of 5 times per second. The salts were purchased separately in their simplest form from Sigma–Aldrich (> 98.5% purity) and mixed mechanically to obtain the 4 different compositions listed in Table 1. Differences in the experimental temperature ranges are due to the respective melting points. The nitrate mixture starts to decompose at 560 °C [13], and is only used up to 500 °C in this study.

Table 1. Composition and properties of salts used in the experiments.

Molten salts composition (wt %)	Experiment temperatures	Melting point	Reference for melting point
LiF–NaF–KF (29.2–11.7–59.1)	475 – 600°C	454 °C	[15]
Li_2CO_3–Na_2CO_3–K_2CO_3 (31.7–33.7–34.7)	450 – 600°C	397 °C	[9]
$ZnCl_2$–KCl (68.0–32.0)	400 – 600°C	181 °C	[20]
$NaNO_3$–KNO_3 (60.0–40.0)	400 – 500°C	220 °C	[13]

200 g of pre–dried salt mixture was filled in a nickel crucible (H = 190 mm, ID = 52 mm) placed inside a stainless steel reactor (H = 200 mm, ID = 62 mm) that was externally heated by an electric furnace (Figure 1). Nickel was chosen for the inner crucible because it is more resistant to corrosion by molten salts.[14] When the heating was started, inert gas (Ar) was continuously flowed into the reactor through a nickel tube (4 mm) to ensure an oxygen–free atmosphere. The salt temperature was controlled by a submerged type K thermocouple. Once the salt was completely melted, the nickel tube was submerged in the melt to give turbulent mixing and a homogeneous temperature throughout the reactor. Turbulent mixing enhances the heat transfer from the salt to the wood particles in the pyrolysis process.

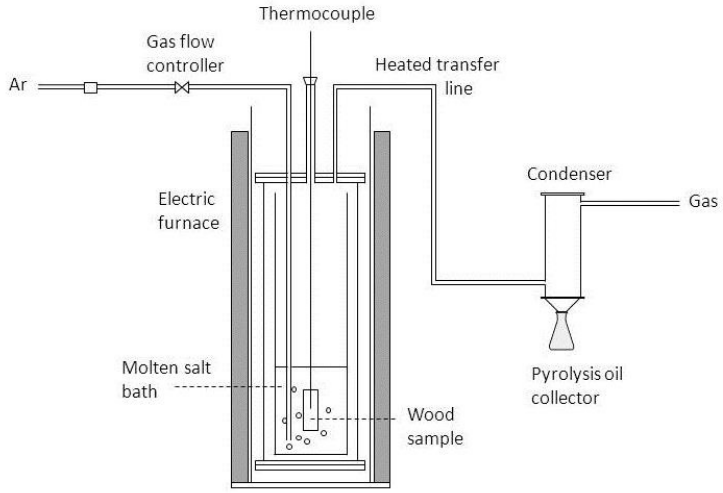

Figure 1. Experimental setup for recording the centre temperature of beech wood particles (d = 3.5 mm) in molten salt pyrolysis.

When the melt was stabilized at the desired temperature, the beech wood particles were introduced to the reactor manually through the top of the sealed reactor. It was ensured that the samples were completely immersed in the molten salt bath throughout the whole experiment. Each experiment was performed at least in triplicate, giving acceptable reproducibility. The flow rate of Ar was set to 2 L/min during the experiments to ensure removal of the produced pyrolysis vapors in less than 3 seconds. The vapors were led out of the reactor through a 4 mm heated transfer line (450 °C) made of stainless steel. The system was connected to a water cooled condenser, but the small samples in this study did not provide enough pyrolysis oil for accurate yield measurements. The non–condensable gases were vented off.

3. Results and discussions

3.1. Temperature profiles and definitions of characteristic points

The temperature measurements were used to construct temperature profiles and calculate heating rates. The temperature profiles at the particle center at reactor temperature T = 500 °C are shown in Figure 2a, where one representative curve is chosen for each salt mixture. Figure 2b shows the temperature profile and corresponding heating rate in FLiNaK at 475 °C, where several characteristic points stand out clearly.

It is clear that the salt mixtures have different effects on the thermal behavior of the wood samples. The temperature profile for the nitrate mixture is very different from the others; a sudden increase in temperature is observed with a maximum much higher than the reactor temperature. It is believed that the salt is reacting exothermically with the components in the wood sample. Carbon is one of the products from wood pyrolysis, and nitrates are reduced by this according to Eqs. (1) and (2) (simulations performed in HSC Chemistry software [21]).

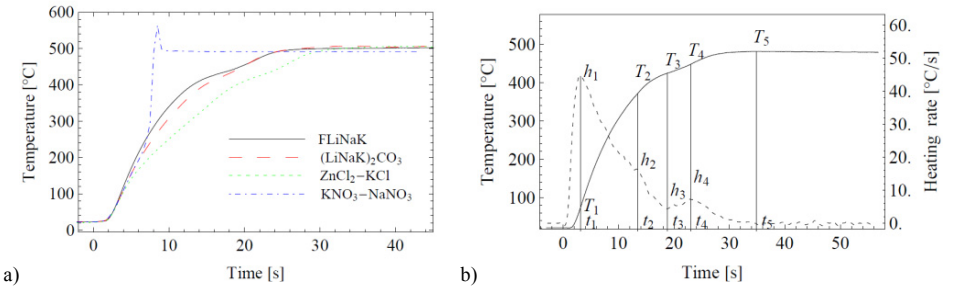

Figure 2.(a) Temperature profiles at the center of beech wood particles (d = 3.5 mm) at reactor temperature T = 500 °C in FLiNaK (black), $(LiNaK)_2CO_3$ (red), $ZnCl_2$–KCl (green), and KNO_3–$NaNO_3$ (blue); (b) Temperature profile and calculated heating rate at the center of beech wood (d = 3.5 mm) in FLiNaK pyrolysis at reactor temperature T = 475 °C.

$$2KNO_3(l) + C \leftrightarrow CO_2(g) + 2KNO_2(l), \qquad \Delta G_{500°C} = -311.86\ kJ/mol \quad (1)$$

$$2NaNO_3(l) + C \leftrightarrow CO_2(g) + 2NaNO_2(l), \qquad \Delta G_{500°C} = -562.09\ kJ/mol \quad (2)$$

A similar pattern is observed for the other reactor temperatures, and the results for this salt are excluded from further analyses since the characteristic pyrolysis points are not clear. For the remaining salts, the shape of both the temperature profiles and heating rates are qualitatively the same for all the investigated reactor temperatures.

The characteristic points shown in Figure 2b are briefly described in Table 2. We have used the same definitions as in our previous study, where we have also included more thorough descriptions.[16] The characteristic points were originally proposed by Di Blasi and Branca in their study of pyrolysis of cylindrical beech wood particles (L = 20 mm, d = 2 – 10 mm) in a hot sand bed (T = 534 °C) fluidized by nitrogen.[17]

Table 2. Description of characteristic points during pyrolysis of beech wood particles.

Characteristic points	Description
h_1 / t_1 /T_1	Maximum heating rate. This is measured right before any reactions occur. After this point, degradation starts in the outer part of the particle and inward heat transfer is hindered.
h_2 / t_2 /T_2	Point of high variation. This indicates the beginning of the endothermic degradation of cellulose and hemicellulose at the particle center.
h_3 / t_3 / T_3	Local minimum of heating rate. This point represents the main occurrence of degradation of cellulose and hemicellulose, and T_3 may be regarded as the effective pyrolysis temperature.
h_4 / t_4 / T_4	Local maximum of heating rate. The exothermic degradation of lignin – which happens over a wider temperature range than cellulose and hemicellulose – starts to slow down. At this point, the conversion is about 95%.
t_5 / T_5	Maximum temperature. The conversion process is practically terminated, and t_5 may be regarded as the total devolatilization time.

3.2. Reaction temperatures and heating rates

The effect of reactor temperature (400 – 600 °C) on the characteristic temperatures in molten salt pyrolysis is shown in Figure 3. For T_1 there is a relatively high scatter in the observations. The high heating rates at this point (Figure 4) makes it difficult to evaluate precise corresponding temperatures. Since the variation within one salt is greater than the variation between the salts, it is not possible to say if there are differences between the salt mixtures. The other characteristic temperatures are more consistent. They are slightly, but not significantly, lower for $ZnCl_2$–KCl. The values are comparable to a corresponding study in fluidized sand bed by Di Blasi and Branca [17], indicating that the heat transfer medium is of less importance to the reaction temperatures. For T_2 and T_3 there is only a weak dependence on reactor temperature, with values in the range 352 – 386 and 404 – 438 °C, respectively.

These temperatures are associated with the beginning and the main occurrence of cellulose and hemicellulose degradation. The reactions are known to occur at a narrow temperature range [22], and depend more on particle size [16] than heat transfer medium. T_4 is related to the degradation of lignin. This happens over a wider temperature range [23], and is more dependent on the reactor temperature than the other characteristic temperatures. An increase in T_4 from 435 to 522 °C is observed as the reactor temperature is increased from 450 to 600 °C.

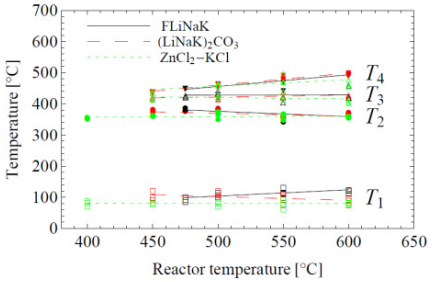

Figure 3. Characteristic temperatures at the center of beech wood particles (d = 3.5 mm) as functions of the reactor temperature in FLiNaK (black), $(LiNaK)_2CO_3$ (red), and $ZnCl_2$–KCl (green).

The characteristic heating rates (h_1 – h_4) as a function of reactor temperature are shown in Figure 4. All the heating rates show an increasing trend with increasing reactor temperature. The maximum heating rate (h_1) is of special interest because it is measured before any reactions occur, and this is where variations between heat transfer media are shown. Although there is some scatter in the observations, it is clear that FLiNaK generally has higher values (46 – 56 °C/s), followed by $(LiNaK)_2CO_3$ (38 – 52 °C/s) and then $ZnCl_2$–KCl (35 – 43 °C/s). The other characteristic heating rates show a strong dependence on reactor temperature; h_2 increases from 8 to 31 °C/s, h_3 from 1 to 20 °C/s, and h_4 from 4 to 43 °C/s. Variations between the salts are, however, negligible.

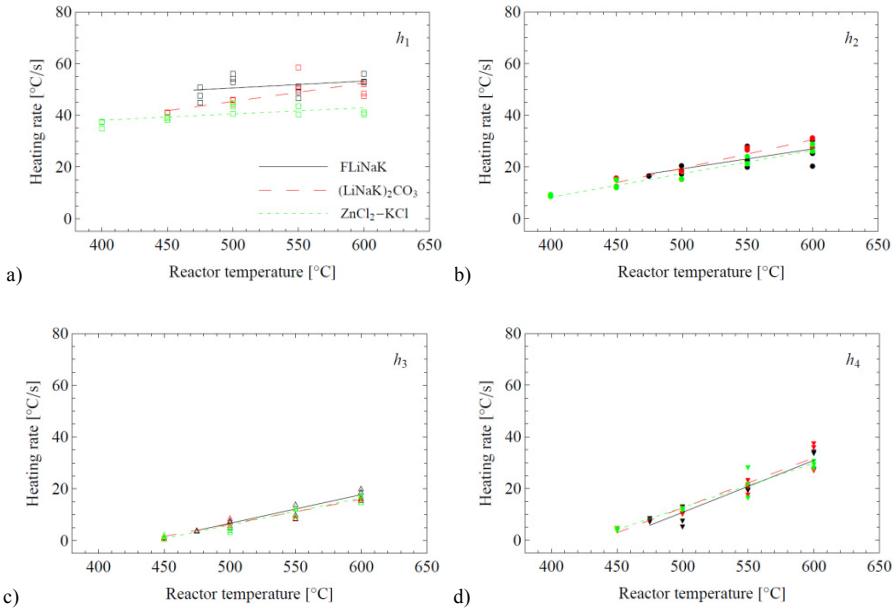

Figure 4. Characteristic heating rates at the center of beech wood particles (d = 3.5 mm) as functions of the reactor temperature in FLiNaK (black), $(LiNaK)_2CO_3$ (red), and $ZnCl_2$–KCl (green).

3.3. Devolatilization times

Prediction of the total devolatilization time in pyrolysis is important for reactor design. Several definitions are used in literature; measurements of gas evolution [24], rate of weight loss [25], or temperature history [26]. Based on the definitions previously introduced (Figure 2b), t_5 could be regarded as the total devolatilization time. However, precise evaluation of t_5 is difficult in this study, because the maximum temperature T_5 cannot be distinguished from small temperature oscillations associated with structural changes or measurement errors for such small particles. We have instead chosen to use t_4 for the evaluation of the devolatilization time to allow for comparison between salt mixtures and reactor temperatures. This corresponds to the second local maximum in the heating rate at the particle center, and the conversion is about 95%.[26]

Figure 5a shows t_4 as a function of the reactor temperature. Values for FLiNaK and $(LiNaK)_2CO_3$ are comparable for all reactor temperatures, while the pyrolysis process takes longer time in $ZnCl_2$–KCl. However, the differences diminish as the bed temperature is increased, and for reactor temperature T = 600 °C there are no significant differences. A common empirical correlation for the devolatilization time is the power–law relation $t_{dev} = Ad^n$, where A and n are fitted to match the experimental data. This was originally proposed for coal particles [27], but has also been shown to be applicable for pyrolysis of wood particles.[17, 24, 28] Values for n typically range between 1 and 2, depending on external or internal heat– and mass–transfer control.[29] Factors such as bed temperature, sample varieties, oxygen concentration, etc., are usually incorporated in the parameter A.[27] In our previous study [16] we found n = 1.05 for cylindrical beech wood particles with diameters between 1 and 8 mm in FLiNaK at 500 °C. We continue to use this value for n, and focus on the parameter A in the following. We have constructed an Arrhenius plot of ln(A) as function of $1000/T_{reactor}$ for each salt mixture (Figure 5b), and found that A depends exponentially on reactor temperature with the relations given in Table 3. This is in agreement with the results reported by other researchers for both coal [27] and wood.[17, 28]

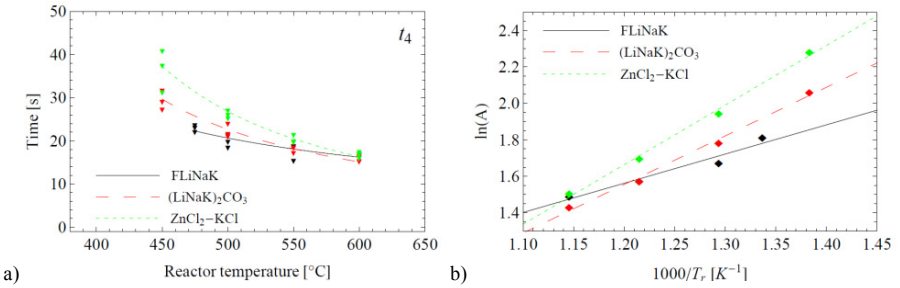

Figure 5. (a) Characteristic heating times for beech wood particles (d = 3.5 mm) as functions of the reactor temperature in FLiNaK (black), $(LiNaK)_2CO_3$ (red), and $ZnCl_2$–KCl (green). (b) Effect of reactor temperature on the correlation parameter A for the devolatilization time for pyrolysis of beech wood particles (d = 3.5 mm) in FLiNaK (black), $(LiNaK)_2CO_3$ (red), and $ZnCl_2$–KCl (green).

The R^2 values for the regression analysis are very good (Table 3), especially for $(LiNaK)_2CO_3$ and $ZnCl_2$–KCl. We have calculated the corresponding activation energies (Table 3), and these are in the same range as found by other researchers.[17, 27] The values are quite low on chemical kinetic scales, indicating heat transfer being the controlling mechanism in the process.[30]

Table 3. Correlation parameter A and corresponding values for the activation energy of beech wood particles in molten salt pyrolysis.

Molten salt	A	R^2	Corresponding activation energy
FLiNaK	$0.698e^{1600/T}$	95.98	13.3 kJ/mol
$(LiNaK)_2CO_3$	$0.194e^{2662/T}$	99.28	22.1 kJ/mol
$ZnCl_2$–KCl	$0.105e^{3264/T}$	99.51	27.4 kJ/mol

4. Conclusions

The pyrolytic behavior of cylindrical beech wood particles (L = 30 mm, d = 3.5 mm) in FLiNaK, $(LiNaK)_2CO_3$, $ZnCl_2$–KCl, and KNO_3–$NaNO_3$ at temperatures between 400 to 600 °C was investigated. Temperature profiles were made based on temperature measurements at the particle center during pyrolysis reactions, and these were used to evaluate the reaction temperatures, heating rates, and devolatilization times.

The nitrate mixture was not suitable for pyrolysis. The temperature profiles differed greatly from the others with a sudden increase in temperature and a maximum much higher than the reactor temperature. This indicates that the salts react exothermic with the carbon formed in the process, also supported by large negative Gibbs free energies for simulated reactions in HSC Chemistry software. Although nitrates have previously shown good heat transfer performance in storage of solar energy [13] and in vacuum pyrolysis [12], these studies do not involve direct contact with carbon containing material.

The characteristic reaction temperatures are slightly, but not significantly, lower for $ZnCl_2$–KCl. The main degradation of cellulose and hemicellulose (T_3) show a weak dependence on reactor temperature (404 – 438 °C), but a stronger dependence is observed for T_4 (435 – 522 °C), which is associated with the degradation of lignin. The highest heating rate (h_1) is measured before any reactions start. Some scatter exists in the observations, but it is still clear that FLiNaK generally has higher values (46 – 56 °C/s), followed by $(LiNaK)_2CO_3$ (38 – 52 °C/s) and then $ZnCl_2$–KCl (35 – 43 °C/s). The other characteristic heating rates are comparable for the salts, but they all depend strongly upon reactor temperature. The devolatilization time t_4 (corresponding to conversion of about 95%) is found to follow the empirical power–law relation $t_{dev} = Ad_p^n$. Arrhenius plots were constructed for each salt mixture to show that A depends exponentially upon temperature. The plots were in good agreement with experimental results, with R^2 values above 96%. Corresponding activation energies were calculated to be in the range from 13.3 to 27.4 kJ/mol, indicating heat transfer control rather than kinetic control in the decomposition process.

The results show that all though the highest heating rate and devolatilization times are affected by the external heating, the heat transfer media is of less importance to reaction temperatures and the remaining heating rates.

References

[1] Bridgwater AV. Review of fast pyrolysis of biomass and product upgrading. *Biomass & Bioenergy* 2012; 38(0): 68-94.

[2] Venderbosch RH, Prins W. Fast pyrolysis technology development. *Biofuels, Bioproducts & Biorefining* 2010; 4(2): 178-208.

[3] Lovering DG. *Molten salt technology*. Plenum Press;1982.

[4] Nygård HS, Olsen E. Review of thermal processing of biomass and waste in molten salts for production of renewable fuels and chemicals. *International Journal of Low-Carbon Technologies* 2012; 7(4): 318-324.

[5] Yoshida S, Matsunami J, Hosokawa Y., Yokota O., Tamaura Y. Coal/CO2 gasification system using molten carbonate salt for solar/fossil energy hybridization. *Energy & fuels* 1999; 13(5): 961-964.

[6] Matsunami J, Yoshida S, Oku Y, Yokota O, Tamaura Y, Kitamura M. Coal gasification by CO2 gas bubbling in molten salt for solar/fossil energy hybridization. *Solar Energy* 2000; 68(3): 257-261.

[7] Matsunami J, Yoshida S, Oku Y, Yokota O, Tamaura Y, Kitamura M. Coal gasification with CO2 in molten salt for solar thermal/chemical energy conversion. *Energy* 2000; 25(1): 71-79.

[8] Adinberg R, Epstein M, Karni J. Solar Gasification of Biomass: A Molten Salt Pyrolysis Study. *Journal of Solar Energy Engineering* 2004; 126(3): 850-857.

[9] Hathaway BJ, Davidson JH, Kittelson DB. Solar Gasification of Biomass: Kinetics of Pyrolysis and Steam Gasification in Molten Salt. *Journal of Solar Energy Engineering* 2011; 133(2): 021011-1 – 021011-9.

[10] Sada E, Kumazawa H, Kudsy M. Pyrolysis of lignins in molten salt media. *Industrial & Engineering Chemistry Research* 1992; 31(2): 612-616.

[11] Kudsy M, Kumazawa H. Pyrolysis of kraft lignin in the presence of molten ZnCl2-KCl mixture. *The Canadian Journal of Chemical Engineering* 1999; 77(6): 1176-1184.

[12] Roy C, Morin D, Dubé F. The biomass PyrolycyclingTM process. In: Kaltschmidt M, Bridgwater AV, editors. *Biomass Gasification and Pyrolysis: State of the Art and Future Prospects*, UK: CPL Press; 1997, p. 307-315.

[13] Mao A, Park JH, Han GY, Seo T, Kang Y. Heat transfer characteristics of high temperature molten salt for storage of thermal energy. *Korean Journal of Chemical Engineering* 2010; 27(5): 1452-1457.

[14] Olson LC, Ambrosek JW, Sridharan K, Anderson MH, Allen TR. Materials corrosion in molten LiF–NaF–KF salt. *Journal of Fluorine Chemistry* 2009; 130(1): 67-73.

[15] Williams D. Assessment of candidate molten salt coolants for the NGNP/NHI Heat-Transfer Loop. ORNL/TM-2006/69, *Oak Ridge National Laboratory*, Oak Ridge, Tennessee, 2006.
[16] Nygård HS, Danielsen F, Olsen E. Thermal History of Wood Particles in Molten Salt Pyrolysis. *Energy & Fuels* 2012; 26(10): 6419-6425.
[17] Di Blasi C, Branca C. Temperatures of Wood Particles in a Hot Sand Bed Fluidized by Nitrogen. *Energy & Fuels* 2003; 17(1): 247-254.
[18] Kersten SRA, Wang X, Prins W, van Swaaij WPM. Biomass Pyrolysis in a Fluidized Bed Reactor. Part 1: Literature Review and Model Simulations. *Industrial & Engineering Chemistry Research* 2005; 44(23): 8773-8785.
[19] Grønli MG. A Theoretical and Experimental Study of the Thermal Degradation of Biomass. PhD thesis, *Norwegian University of Science and Technology* 1996.
[20] Jiang H, Ai N, Wang M, Ji D, Ji J. Experimental Study on Thermal Pyrolysis of Biomass in Molten Salt Media. *Electrochemistry* 2009; 77(8): 730-735.
[21] HSC Chemistry software, version 6.1.
[22] Di Blasi C, Branca C. Kinetics of Primary Product Formation from Wood Pyrolysis. *Industrial & Engineering Chemistry Research* 2001; 40(23): 5547-5556.
[23] Antal MJ Jr, Varhegyi G. Cellulose Pyrolysis Kinetics: The Current State of Knowledge. *Industrial & Engineering Chemistry Research* 1995; 34(3): 703-717.
[24] de Diego LF, García-Labiano F, Abad A, Gayán P, Adánez J. Modeling of the Devolatilization of Nonspherical Wet Pine Wood Particles in Fluidized Beds. *Industrial & Engineering Chemistry Research* 2002; 41(15): 3642-3650.
[25] Di Blasi C, Hernandez EG, Santoro A. Radiative Pyrolysis of Single Moist Wood Particles. *Industrial & Engineering Chemistry Research* 2000; 39(4): 873-882.
[26] Di Blasi C, Branca C, Santoro A, Hernandez EG. Pyrolytic behavior and products of some wood varieties. *Combustion and Flame* 2001; 124(1–2): 165-177.
[27] Ross DP, Heidenreich CA, Zhang DK. Devolatilisation times of coal particles in a fluidised-bed. *Fuel* 2000; 79(8): 873-883.
[28] Gaston KR, Jarvis MW, Pepiot P, Smith KM, Frederick WJ, Nimlos MR. Biomass Pyrolysis and Gasification of Varying Particle Sizes in a Fluidized-Bed Reactor. Energy & Fuels 2011; 25(8): 3747-3757.
[29] Kanury AM. Combustion Characteristics of Biomass Fuels. *Combustion Science and Technology* 1994; 97(4-6): 469-491.
[30] Jia L, Becker HA, Code RK. Devolatilization and char burning of coal particles in a fluidized bed combustor. *The Canadian Journal of Chemical Engineering* 1993; 71(1): 10-19.